Burns & Trauma, 2021, 9, tkab033
https://doi.org/10.1093/burnst/tkab033
Research Article

Research Article

Co-administration of platelet-rich plasma and small intestinal submucosa is more beneficial than their individual use in promoting acute skin wound healing

Xiaoxuan Lei[1,2,†], Liuhanghang Cheng[1,2,†], Yu Yang[2], Mengru Pang[2], Yunqing Dong[2], Xuanru Zhu[2], Caihong Chen[2], Zexin Yao[2], Gang Wu[1,3,*], Biao Cheng[2,*] and Tymour Forouzanfar[1]

[1]Department of Oral and Maxillofacial Surgery/Pathology, Amsterdam UMC and Academic Center for Dentistry Amsterdam (ACTA), Vrije Universiteit Amsterdam, Amsterdam Movement Science, Amsterdam, 1081HV, The Netherlands, [2]Department of Burn and Plastic Surgery, General Hospital of Southern Theater Command, Guangzhou, 510030, China and [3]Department of Oral Implantology and Prosthetic Dentistry, Academic Center for Dentistry Amsterdam (ACTA), University of Amsterdam (UvA) and Vrije Universiteit Amsterdam (VU), Amsterdam, 1081LA, The Netherlands

*Correspondence. Gang Wu, Email: g.wu@acta.nl and Biao Cheng, Email: chengbiaocheng@163.com

[†]These authors contributed equally to this work.

Received 5 February 2021; Revised 14 July 2021; Editorial decision 19 July 2021

Abstract

Background: Acute skin wounds may compromise the skin barrier, posing a risk of infection. Small intestinal submucosa (SIS) is widely used to treat acute and chronic wounds. However, the efficacy of SIS to accelerate wound healing still needs to be improved to meet clinical demands. To tackle this problem, platelet-rich plasma (PRP) is used due to its potency to promote proliferation, migration and adhesion of target cells. In this study, we applied PRP and SIS to skin wounds to explore their effects on wound healing by evaluating re-epithelialization, collagen production, angiogenesis and the inflammatory response.

Methods: A 1 × 1-cm full-thickness skin defect was established in mice. Sixty mice were divided into four treatment groups: PRP + SIS, PRP, SIS and control. On days 3, 5, 7, 10 and 14 post-surgery, tissue specimens were harvested. Haematoxylin and eosin, Masson's trichrome, immunohistochemical and immunofluorescence double staining were used to visualize epidermal thickness, collagen and vascular regeneration and inflammation.

Results: Wound contraction in the PRP and PRP + SIS groups was significantly greater, compared with the other groups, on days 3 and 5 post-surgery. A histological analysis showed higher collagen expression in the PRP and PRP + SIS groups on day 7, which was associated with a thicker epidermal layer on day 14. In addition, immunohistochemical staining showed that CD31-positive blood vessels and vascular endothelial growth factor expression in the PRP + SIS and PRP groups were significantly higher, compared with the control group. Furthermore, immunofluorescence double staining showed that the number of M1 and M2 macrophages in the PRP + SIS and PRP groups was higher, compared with the control and SIS groups alone, on day 3. However, on day 7, the number of M1 macrophages dramatically decreased in the PRP + SIS and PRP groups. The ratio of M2 to M1 macrophages in the PRP + SIS and PRP groups was 3.97 and 2.93 times that of the control group and 4.56 and 3.37 times that of the SIS group, respectively.

© Crown copyright 2021.
This article contains public sector information licensed under the Open Government Licence v3.0 (https://www.nationalarchives.gov.uk/doc/open-government-licence/version/3/).

Downloaded from https://academic.oup.com/burnstrauma/article/doi/10.1093/burnst/tkab033/6446275 by guest on 08 June 2022

Conclusion: Co-administration of SIS and PRP has a better effect on promoting angiogenesis, re-epithelialization and collagen regeneration in managing acute wound healing than either agent alone.

Key words: Small intestinal submucosa, Platelet-rich plasma, Full-thickness skin defect, M1 macrophages, M2 macrophages, Animal model, wound healing, skin

Highlights

- This study revealed that applying PRP to acute wounds facilitates the transition of M1 into M2 macrophages.
- The preparation of PRP is recommended acoording to the author's experience.
- Co-administration of SIS and PRP has a better effect on promoting angiogenesis, re-epithelialization and collagen regeneration than either agent alone.

Background

The skin, as a protective barrier, plays an important role in retaining water, maintaining electrolytes and preventing the invasion of pathogens. The barrier function of the skin is compromised by acute skin wounds caused by trauma, surgical procedures and burns, which may lead to a series of complications, such as infection [1]. In patients with chronic diseases, such as diabetes mellitus, wounds fail to heal and can become chronic. Therefore, it is important to accelerate wound healing and recover the structural integrity and functionality of the skin.

Wound healing is a continuous pathophysiological process of tissue regeneration, which consists of four consecutive phases: (1) coagulation and haemostasis, (2) inflammation, (3) proliferation and (4) wound remodelling [2]. Immediately after an acute injury, platelet aggregation and blood clot formation at wound sites are triggered by release of clotting factors [3]. Platelet activation can release growth factors, such as platelet-derived growth factor (PDGF) and transforming growth factor-β1 (TGF-β1), which act to stimulate wound healing by attracting and recruiting neutrophils, macrophages and endothelial cells [3, 4]. Macrophages are one of the main cell types that participate in inflammation and can be divided into two distinct phenotypes: (1) classically activated and pro-inflammatory M1 macrophages and (2) alternatively activated and anti-inflammatory M2 macrophages [5]. Within 3–5 days after injury, M1 macrophages infiltrate wound areas and phagocytose pathogens and senescent cells. M1 macrophages are typically associated with pro-inflammatory events, such as the production of interleukin-6 (IL-6) and tumour necrosis factor-α (TNF-α) [6]. At 5–7 days after injury, M1 macrophages transition into M2 macrophages, which gradually dominate wound sites [7]. M2 macrophages express high levels of TGF-β1 and vascular endothelial growth factor-α (VEGF-α) to promote angiogenesis and re-epithelialization. M2 macrophages also stimulate the synthesis and secretion of collagen fibres and matrix proteins from fibroblasts [8]. Continuous efforts have been made to develop new materials that target these biological events to promote healing of acute skin wounds. In recent years, biomaterials, bioactive factors and stem cells have shown promising prospects for wound healing.

One such material to promote skin wound healing is small intestinal submucosa (SIS), which is derived from the mucosal and muscle layers of the intestine. SIS consists of collagens, glycosaminoglycans (GAGs), proteoglycans, fibronectins and hyaluronic acid (HA) [9], as well as a series of active growth factors, including TGF-β, epidermal growth factor (EGF) and VEGF [10]. SIS has low antigenicity, good histocompatibility and proper degradability. SIS bears low porosity and thus has a limited capacity for water to flow through, which may serve as a protective barrier to prevent wound bed dehydration [11, 12]. SIS can promote proliferation, migration and attachment of fibroblasts, keratinocytes and endothelial cells *in vitro* [13, 14]. SIS is also widely applied to treat various wound types *in vivo* [15, 16]. However, its efficacy in accelerating wound healing still needs to be improved to meet clinical demands [17]. Thus, it is essential to seek suitable bioactive agents to achieve a better therapeutic effect.

Platelet-rich plasma (PRP) is an inherently safe and easily accessible platelet concentrate derived from autologous blood [18]. Platelet activation and degranulation can release large amounts of bioactive factors, including growth factors and exosomes [18, 19]. The major growth factors in PRP are PDGF, TGF-β, VEGF and EGF, which stimulate and promote proliferation, migration and adhesion of target cells, such as fibroblasts, epithelial cells and endothelial cells [20–22]. PRP promotes healing of various wound types, including acute wounds [23, 24]. In addition, exosomes derived from PRP can effectively induce proliferation and migration of endothelial cells and fibroblasts to improve angiogenesis and re-epithelialization in chronic wounds. This occurs through activation of Yes-associated protein (YAP) signalling [19]. Furthermore, platelets in PRP contain pro- and anti-inflammatory factors that participate in macrophage polarization [25]. However, proteases can cleave molecules, leading to rapid degradation of platelet-activating factors [26], and administration of PRP liquid on wounds extremely gets losses. This situation inspired us to co-administer SIS and PRP, since SIS may provide a slow delivery system for PRP to exert a better effect on wound healing.

Downloaded from https://academic.oup.com/burnstrauma/article/doi/10.1093/burnst/tkab033/6446275 by guest on 08 June 2022

In the present study, a full-thickness skin defect model was established in mice. PRP and SIS were applied to skin wounds to explore the effects of wound healing at different stages. Wound healing percentage, re-epithelialization collagen production, angiogenesis and the inflammatory response were assessed. Our study aimed to explore effective treatments for wound healing and analyse the biological mechanisms, to provide a beneficial reference for clinical application.

Methods

PRP/SIS preparation

PRP was prepared from an autologous blood sample voluntarily provided by a healthy adult (female, aged 26 years) at the General Hospital of Southern Theater Command. The platelet concentration of whole blood was 191×10^9/l. Blood was centrifuged for 10 minutes at 600 *g* to collect the plasma derived from the upper and middle layers. Subsequently, plasma was centrifuged again for 20 minutes at 1500 *g*. The upper platelet-deficient plasma layer was separated, and the remaining PRP layer was activated using 10% calcium gluconate (clinical use) at a ratio of 9:1 (v/v). The platelet concentration of PRP was 887×10^9/l.

SIS powder was obtained from Guangzhou Sinoregen Medical Materials Co. Ltd (China). Before application, SIS powder was thoroughly mixed with PRP and 0.9% sodium chloride (NaCl) at a volume ratio of 1:1 (v/v) through three-way pipes (B. Braun Inc., Germany) and formed into a paste. The four treatment groups were as follows: G1 (no PRP, no SIS); G2 (PRP alone); G3 (SIS alone); and G4 (SIS + PRP).

Acute *in-vivo* wound model

Sixty male C57 mice aged 6–8 weeks and weighing 22–28 g were obtained from the Animal Research Centre of Guangdong (China). The animal experiment was approved by the Animal Care Committee of General Hospital of Southern Theater Command (animal ethics approval number: 2018030601).

First, 1% pentobarbital sodium (5 ml/kg) was administered to mice via intraperitoneal injection to induce anaesthesia. After induction of anaesthesia, the dorsal hair of mice was shaven and sterilized with iodophor. A 1 × 1-cm full-thickness skin defect in the dorsal area of each mouse was made, using a square punch biopsy instrument. Four treatments were randomly applied to the wounds, and each wound was treated with a 0.5-ml dose of the respective treatment each day. On days 3, 5, 7, 10 and 14 post-surgery, three mice were randomly sacrificed from each group at each time point and tissue specimens were harvested.

Wound contraction

On days 0, 3, 5, 7, 10 and 14 post-surgery, wounds were photographed with a Nikon digital camera (Japan) and the wound area was measured using Image J software. Wound contraction (%) was calculated according to the following formula: wound contraction (%) = $[(A_0 - A_x) \div A_0] \times 100\%$, where A_0 represents the initial wound area and A_t represents the wound area at each time point [27].

Histological staining

Haematoxylin and eosin (H&E) staining Tissue specimens were fixed in 4% paraformaldehyde for 48 hours and dehydrated step by step in a dehydrator (JJ-12 J; Junjie Electronics Inc., China). Subsequently, samples were embedded, sliced to a thickness of 4 μm and dried in an oven (Shanghai Huitai Instrument Manufacturing Co. Ltd, China) at 65°C for 2 hours. Sections were stained with H&E and photographed using an electron microscope (Olympus BX51; Olympus, Germany). The re-epithelialized area and length were measured and analysed using Image J software. The epithelial thickness was calculated by epithelial area ÷ epithelial length. Five tissue sections in each group were selected to calculate mean ± standard deviation (SD).

Masson's trichrome staining Tissue specimens were dehydrated and stained in sequence with haematoxylin (G1004; ServiceBio Inc., USA) for 5 minutes, ponceau-acid fuchsin solution (G2011; ServiceBio Inc.) for 5 minutes, 1% phosphomolybdic acid (G3472; Solarbio science&tehnology Co., Ltd, China) for 2 minutes and aniline blue (G1071; ServiceBio Inc.) for 5 minutes, and subsequently dehydrated and sealed. Stained sections were photographed using a microscope, and collagen expression was analysed using Image-Pro Plus (Media Cybernetics, Inc. Moldova). The positive expression level of new collagen fibres was calculated according to the following formula: mean optical density (MOD) = integrated option density (IOD) sum ÷ area sum.

Immunohistochemistry

Sections were deparaffinized and blocked in 3% hydrogen peroxide solution for 10 minutes at room temperature. After rinsing in phosphate-buffered saline, sections were incubated overnight at 4°C with antibodies, including rabbit anti-platelet CD31 (GB13063, 1:300; Servicebio Inc.) and mouse anti-VEGF (MA5–13182, 1:100; Thermo Fisher Scientific Co. Ltd, USA). Correspondingly, sections were incubated with secondary goat anti-mouse (G1214, 1:200; ServiceBio Inc.) or goat anti-rabbit (G1213, 1:200; ServiceBio Inc.) antibodies at 37°C for 50 minutes and detected with 3,3′-diaminobenzidine tetrahydrochloride (DAB) solution (G1211; ServiceBio Inc.) for 10 minutes. Nuclei were stained with haematoxylin. All sections were photographed with a microscope, and the area and IOD of VEGF expression were analysed using Image-Pro Plus software. VEGF expression was calculated according to the following formula: MOD = IOD sum ÷ area sum. CD31-positive blood vessels were quantified using Image-Pro Plus software with blind tests. Images from five sections in each group and from five different fields in each section were

Downloaded from https://academic.oup.com/burnstrauma/article/doi/10.1093/burnst/tkab033/6446275 by guest on 08 June 2022

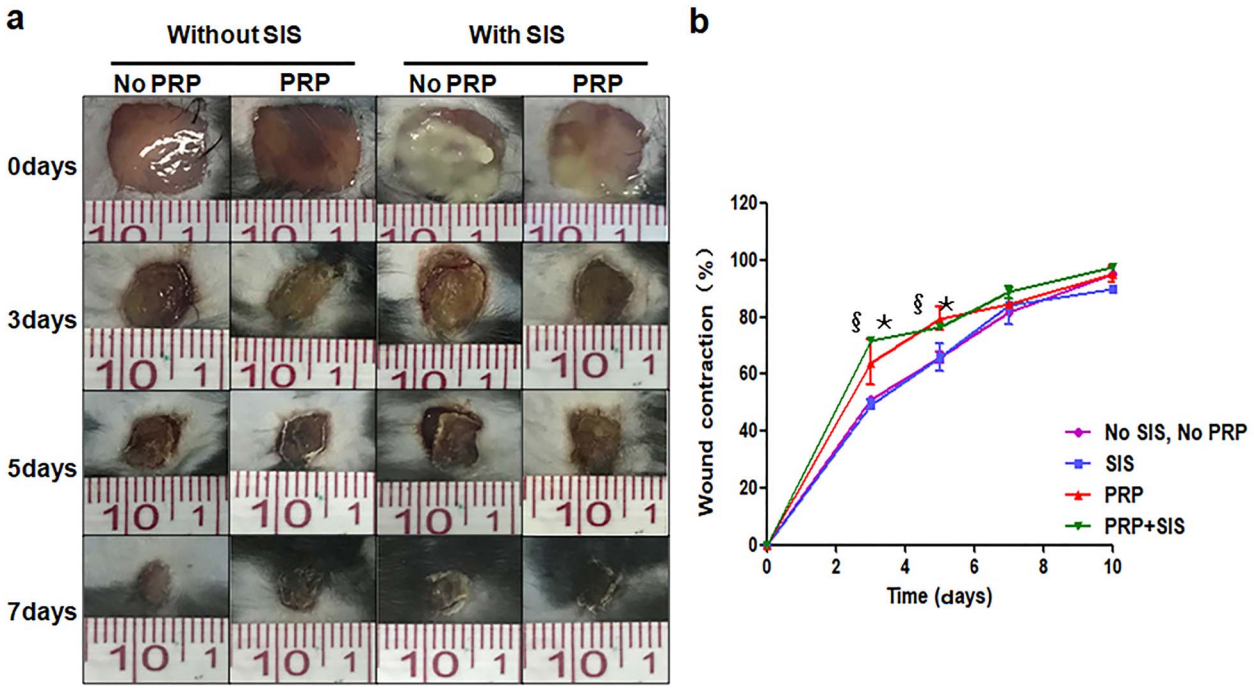


Figure 1. Day 0, 3, 5, 7 after treatment, the dynamic changes of the wound area in four groups. **(a)** Representative images of acute wounds showing that wounds treated with platelet-rich plasma (PRP) alone and PRP + small intestinal submucosa (SIS) presented a smaller wound area compared to the control and SIS alone. **(b)** Wound contraction (%) in each treatment group. On days 3, 7 and 10, the healing percentage of the wounds treated with PRP + SIS was higher compared to the control, SIS alone and PRP alone, while PRP showed superior efficacy on day 5. Data were presented as mean ± standard deviation (SD). §PRP+SIS group and PRP group vs the control group ($p < 0.05$), *PRP+SIS group and PRP group *vs* the SIS group ($p < 0.05$)

submitted to Image-Pro Plus software, and the average value of positive results was automatically counted and calculated.

Immunofluorescence

Immunofluorescence double staining was performed to identify M1 and M2 macrophages [28]. Tissue sections were incubated overnight at 4°C with antibodies against CD68 (GB11067, 1:300; ServiceBio Inc.), CD80 (GB11034, 1:300; ServiceBio Inc.) and CD206 (GB11062, 1:500; ServiceBio Inc.). Correspondingly, sections were incubated with secondary horseradish peroxidase donkey anti-rabbit immunoglobulin G (IgG) antibodies (ab150075, 1:2000; Abcam Trade Co. Ltd, China), and nuclei were stained with DAPI (G1012; Google Biotechnology Co. Ltd, China) for 10 minutes. Stained sections were observed and photographed using a fluorescence microscope (Nikon Eclipse TI-SR; Nikon, Japan). M1 (CD68-positive and CD80-positive) and M2 (CD68-positive and CD206-positive) macrophages were automatically counted and analysed using Image-Pro Plus.

Statistical analysis

SPSS software was used to detect significant differences. All quantitative results were expressed as mean ± SD. Data were analysed using one-way analysis of variance and Bonferroni tests. A p value of <0.05 was considered statistically significant.

Results

Effects of PRP, SIS and PRP + SIS on acute wound contraction

At all selected time points (3, 5, 7 and 10 days post-surgery), wound contraction in the SIS group was similar to that in the control group (Figure 1a). Three and 5 days post-surgery, the closed wound area in the PRP and PRP + SIS groups was significantly more pronounced, compared with the SIS and control groups (Figure 1a). On days 3, 7 and 10, the closed wound area in the PRP + SIS group was the most pronounced among the four groups, while PRP showed superior efficacy only on day 5 (Figure 1b).

Effects of PRP, SIS and PRP + SIS on re-epithelialization and collagen expression

H&E and Masson's trichrome staining were performed to evaluate the effects of PRP + SIS on re-epithelialization (Figure 2a) and collagen expression (Figure 3a), respectively. Fourteen days post-surgery, a quantitative analysis showed that the average thickness of the newly formed epidermal layers in the PRP + SIS and PRP groups was significantly greater, compared with the SIS and control groups (Figure 2b), while no difference was found between the two PRP groups.

Collagen expression was analysed on day 7 post-surgery at wound sites. Treatment with PRP + SIS was associated with the highest collagen expression, which was followed by

Downloaded from https://academic.oup.com/burnstrauma/article/doi/10.1093/burnst/tkab033/6446275 by guest on 08 June 2022

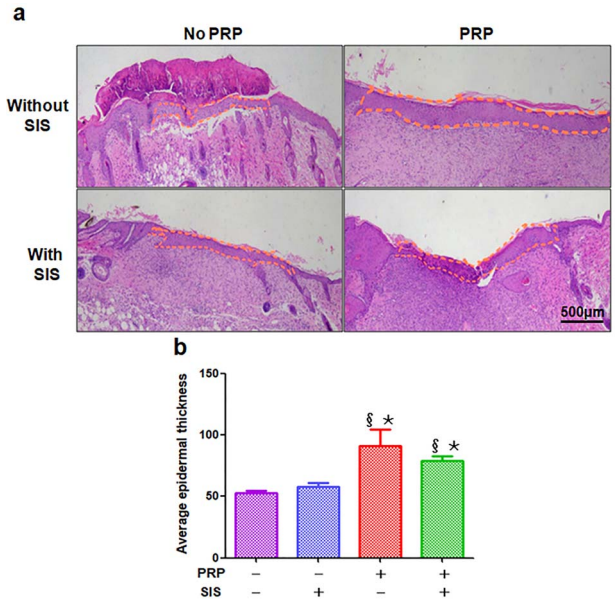


Figure 2. Histological evaluation of epidermal thickness at wound sites. **(a)** Fourteen days post-surgery, the cell layers of newly formed epidermal layer in the PRP and PRP + SIS groups were thicker than those in the control and SIS groups. The yellow curve shows the epidermal regeneration area. Scale bar = 500 μm. **(b)** Quantitative analysis showed that treatment with PRP and PRP + SIS was associated with the greatest thickness of newly formed epidermal layer. §PRP and PRP + SIS groups *vs* control group; *PRP and PRP + SIS groups *vs* SIS group ($p < 0.05$). *PRP* platelet-rich plasma, *SIS* small intestinal submucosa

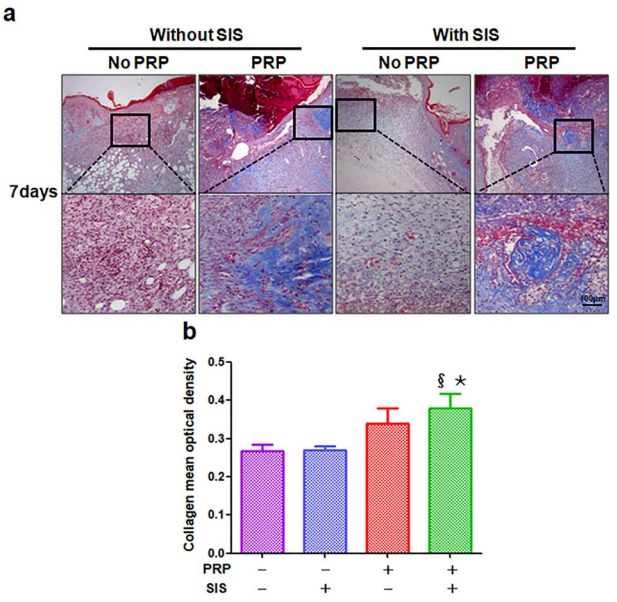


Figure 3. Masson staining evaluation of collagen fibres deposited at the wound sites. **(a)** Seven days post-surgery, there was massive deposition of collagen fibres in the PRP + SIS group. Blue staining represents positive collagen expression. Scale bar = 100 μm. **(b)** Quantitative analysis showed that collagen expression level in the PRP + SIS group was significantly higher compared with the other groups, whilst either SIS or the control intervention did not significantly influence collagen expression. §PRP + SIS group *vs* control group; *PRP + SIS group *vs* SIS group ($p < 0.05$). *PRP* platelet-rich plasma, *SIS* small intestinal submucosa

treatment with PRP alone (Figure 3b). In contrast, the SIS group showed a similar collagen expression to that in the control group. Collagen expression in the PRP + SIS group was significantly higher, compared with the SIS and control groups, while that in the PRP group was not significantly different when compared with the SIS and control groups. There was no significant difference between treatment with PRP + SIS and PRP alone.

Effects of PRP, SIS and PRP + SIS on angiogenesis

To evaluate the effects of PRP, SIS and PRP + SIS on angiogenesis, immunohistochemical staining was performed to detect VEGF as a marker of angiogenesis (Figure 4a), and CD31 as a vascular endothelial cell marker (Figure 5a). On day 14 post-surgery, CD31-positive blood vessels in the PRP + SIS and PRP groups were 2.80 and 2.53 times more abundant compared with the control group, and 2.00 and 1.81 times more abundant compared with the SIS group, respectively, while no significant difference in the number of CD31-positive blood vessels was found between the PRP + SIS and PRP groups (Figure 4b). On day 14 post-surgery, VEGF expression in the PRP + SIS group was significantly higher compared with the control group, while that in the PRP and SIS groups was not significantly different compared with the control group (Figure 5b).

Effects of PRP, SIS and PRP + SIS on macrophage polarization

To investigate the effect of PRP + SIS on macrophage polarization at wound sites, M1 (CD68 and CD80) and M2 (CD68 and CD206) macrophages [29] were stained on days 3 and 7 post-surgery. Three days post-surgery, the number of M1 macrophages in the PRP + SIS (22.3 ± 6.6) and PRP (19.7 ± 3.5) groups was higher compared with the control (10.7 ± 3.1) and SIS (11.7 ± 3.1) groups, while there was no significant difference among all groups (Figure 6c). On day 7 post-surgery, the number of M1 macrophages in the SIS and control groups mildly decreased. In contrast, the number of M1 macrophages in the PRP + SIS and PRP groups significantly decreased to a similar level to that in the SIS and control groups (Figure 6c).

Three days post-surgery, the number of M2 macrophages in the PRP + SIS (53.7 ± 14.4) and PRP (52.3 ± 18.3) groups was significantly higher compared with the control (17.0 ± 4.0) and SIS (19.3 ± 4.2) groups (Figure 6d). Seven days post-surgery, the number of M2 macrophages in the four groups decreased, while the number of M2 macrophages in the PRP + SIS (25.3 ± 5.5) and PRP (23.3 ± 5.7) groups was still significantly greater compared with the control (8.7 ± 1.5) and SIS (9.3 ± 4.9) groups (Figure 6d). On days 3 and 7, the number of M2 macrophages in the PRP + SIS group was slightly higher compared with the PRP group,

Downloaded from https://academic.oup.com/burnstrauma/article/doi/10.1093/burnst/tkab033/6446275 by guest on 08 June 2022

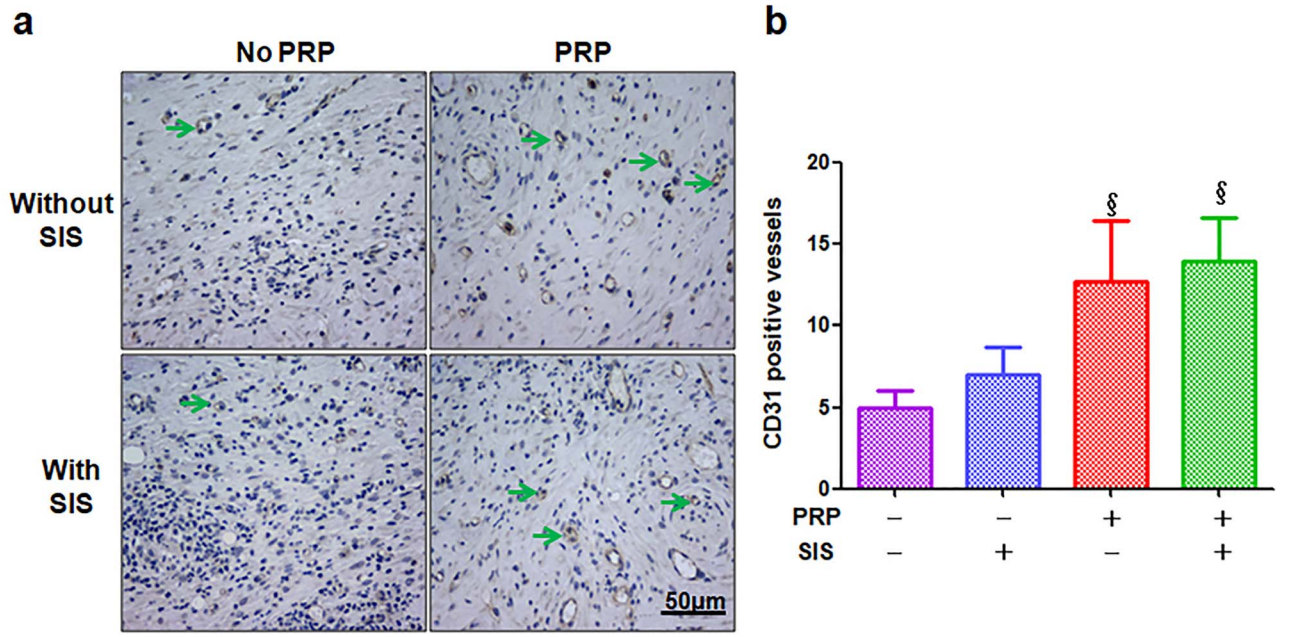


Figure 4. Immunohistochemical evaluation of endothelial cell adhesion molecule-1 (CD31)-positive blood vessels at wound sites. **(a)** Fourteen days post-surgery, the number of CD31-positive blood vessels per microscopic field in the PRP + SIS and PRP groups were 2.80 and 2.53 times that of the control, respectively, and 2.00 and 1.81 times that of the SIS alone group, respectively, as shown by green arrows. Scale bar = 50 μm. **(b)** Quantitative analysis showed that the PRP + SIS group had the highest number of new blood vessels, compared with the other groups. § PRP + SIS group *vs* control group ($p < 0.05$). *PRP* platelet-rich plasma, *SIS* small intestinal submucosa

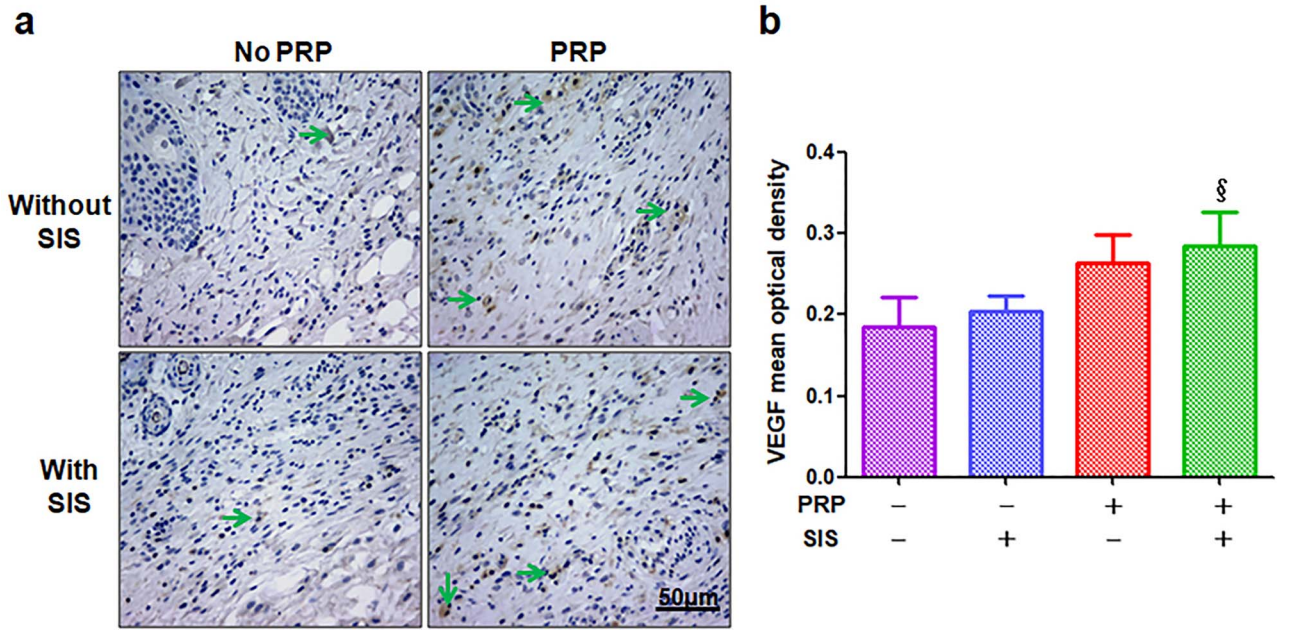


Figure 5. Immunohistochemical evaluation of the expression level of the angiogenic marker vascular endothelial growth factor (VEGF). **(a)** Fourteen days post-surgery, the positive expression level of VEGF was higher in the PRP + SIS group, as shown by green arrows. Scale bar = 50 μm. **(b)** Quantitative analysis showed that VEGF expression in the PRP + SIS group was significantly higher, compared with the control and SIS groups. § PRP + SIS group *vs* control group ($p < 0.05$). *PRP* platelet-rich plasma, *SIS* small intestinal submucosa

with no significant difference observed between the two PRP groups.

Three days post-surgery, the ratio of M2 to M1 macrophages in the PRP + SIS (2.45 ± 0.4) and PRP (2.62 ± 0.3) groups was significantly higher, compared with the SIS (1.7 ± 0.1) and control (1.6 ± 0.1) groups (Figure 6e). On day 7 post-surgery, the ratio of M2 to M1 macrophages in the PRP + SIS and PRP groups increased dramatically and was 3.97 and 2.93 times that of the control group, respectively, and 4.56 and 3.37 times that of the SIS group, respectively (Figure 6e).

Downloaded from https://academic.oup.com/burnstrauma/article/doi/10.1093/burnst/tkab033/6446275 by guest on 08 June 2022

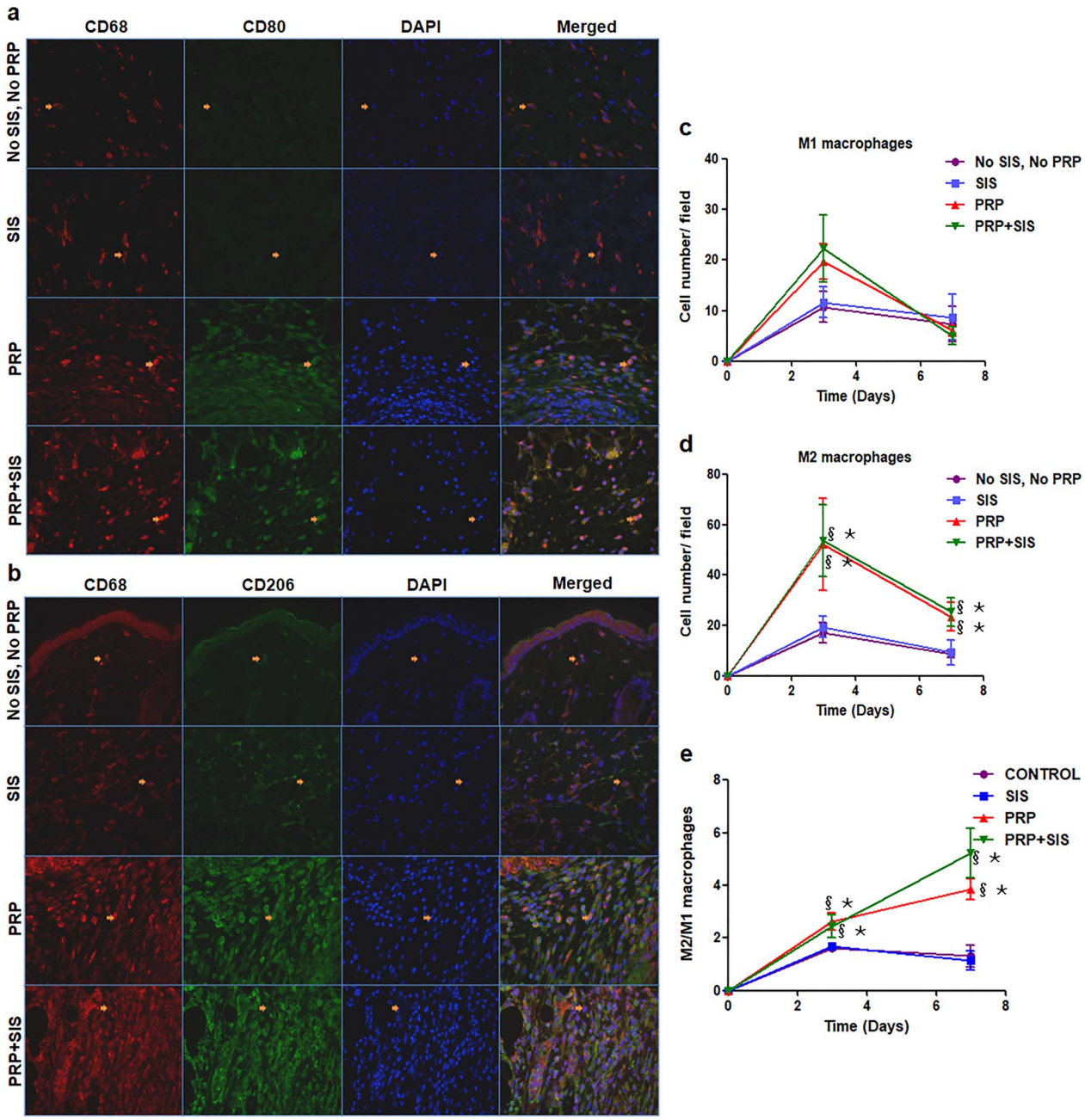


Figure 6. Immunofluorescence double staining of M1 and M2 macrophages at wound sites. **(a)** and **(b)** Representative images of M1 macrophages (CD68, red; CD80, green; nuclei, blue) and M2 macrophages (CD68, red; CD206, green; nuclei, blue) on day 3 post-surgery, as shown by yellow arrows. **(c)** and **(d)** Changes in cell counts of M1 and M2 macrophages in the four groups. On day 3 post-surgery, quantitative analysis showed that the number of M1 and M2 macrophages in the PRP + SIS and PRP groups was higher, compared to the control and SIS alone groups. On day 7, the number of M1 macrophages dramatically decreased in the PRP + SIS and PRP groups and the number of M2 macrophages in the PRP + SIS and PRP groups were significantly higher, compared to the control and SIS alone groups. **(e)** The ratio of M2 to M1 macrophages in the PRP + SIS and PRP groups was significantly higher, compared to the SIS alone and control groups, on days 3 and 7. §PRP and PRP + SIS groups *vs* control group; *PRP and PRP + SIS groups *vs* SIS group ($p < 0.05$). *PRP* platelet-rich plasma, *SIS* small intestinal submucosa

Discussion

The primary function of the skin is to serve as a protective barrier against damage from the external environment. Once damage to the skin occurs, the barrier loses its protective function [30]. It is essential to accelerate wound healing to rapidly reconstruct damaged skin tissue and restore its structural and functional integrity. Our results show that wound contraction was significantly greater with PRP + SIS treatment, compared with the control intervention or SIS alone. Thus, co-administration of PRP and SIS is more

Downloaded from https://academic.oup.com/burnstrauma/article/doi/10.1093/burnst/tkab033/6446275 by guest on 08 June 2022

beneficial than their individual use in promoting acute skin wound healing.

A desirable wound dressing should be developed to promote wound healing. With burns, degloving injuries and chronic wounds, the dermal extracellular matrix (ECM) may be completely absent. SIS, as a biologically derived ECM material that contains major dermal matrix components, has been widely applied to treat acute and chronic wounds by promoting proliferation, migration and attachment of various skin cells [16, 31]. However, an animal study showed that addition of SIS does not significantly promote wound closure in acute full-thickness wounds in dogs when compared with control animals [32]. Our study confirmed that SIS alone was not associated with significantly higher healing efficacy within the 14-day monitoring span. Therefore, optimizing the efficacy of wound healing is of paramount importance. PRP is clinically proven to be safe and effective for wound healing [33], but there has been no clear evidence of its efficacy. One study showed that the effect of PRP is weak due to its short half-life, and local administration should be repeated to achieve wound healing [34, 35]. To overcome this limitation, we applied both PRP and SIS to acute wounds, which resulted in significantly greater wound contraction, compared with SIS alone and with the control intervention, 3 days post-surgery. Such a beneficial effect may be attributed to a host of powerful mitogenic and chemotactic growth factors in PRP. All types of skin cells involved in wound repair are sensitive to growth factors [36, 37] that promote proliferation, migration and adhesion of target cells, such as fibroblasts, epithelial cells and endothelial cells [22, 38]. Furthermore, SIS may serve as a slow-release system for PRP to decelerate its degradation.

In this study, we hypothesized that co-administration of SIS and PRP might achieve better wound healing than application of either agent alone. Considering that the bioactive factors in PRP degrade easily [35], SIS may serve as a slow-release system for PRP. Furthermore, the bioactive agents in PRP may contribute to better wound healing. In our study, co-administration of PRP and SIS yielded a significantly better effect on wound contraction, which supports our hypothesis. However, ideal healing not only focuses on promoting the speed of wound healing, but also improves skin aesthetics and functionality.

In the process of wound healing, it is essential to accelerate the formation of new epidermis and to avoid pathogenic invasion and dehydration. Epidermal cells and keratinocytes migrating from the wound margin undergo a proliferative burst to replace those defected cell layers [39]. Once the wound surface has been covered by a monolayer of keratinocytes, the process of epidermal migration creases and a new stratified epidermis with an underlying basal lamina is re-established [39]. Approximately 1 week after injury, fibroblasts have completely infiltrated into the wound, which are mainly mediated by TGF-β1 and PDGF to synthesize and remodel new collagen [40]. Our results show that co-administration of SIS and PRP was associated with significantly greater epidermal thickness and higher collagen expression, compared with the control and SIS groups, while PRP alone only showed a superior effect in promoting epidermis formation. These results demonstrate that co-administration of SIS and PRP efficaciously stimulated proliferation and migration of skin cells, as well as potentiated their functionality. Such an effect may be primarily attributed to growth factors, including EGF and TGF-β1, in PRP and SIS, which promote proliferation, migration and adhesion of skin cells to enhance re-epithelialization and collagen systhesis [41, 42]. In addition, the wound healing property of exosomes released from PRP is induced by exosomes promoting proliferation and re-epithelialization of fibroblasts through YAP activation [19].

New blood vessel formation takes place during all phases of wound healing to provide a desirable microenvironment for cell growth. A variety of cells, such as endothelial cells and macrophages, as well as angiogenic factors, such as TGF-β1 and VEGF, are involved in the process of angiogenesis [43, 44]. *In vitro*, VEGF is a highly specific mitogen that inhibits endothelial cell apoptosis, promotes endothelial cell proliferation and increases vascular permeability [45]. In this study, co-administration of SIS and PRP yielded the greatest number of CD31-positive blood vessels and showed the highest VEGF expression, which was followed by PRP alone. In contrast, neither SIS alone nor the control intervention promoted angiogenesis. Mechanistically, PRP has direct proliferation-inducing effects on endothelial cells through activation of the phosphatidylinositol 3-kinase (PI3K)/Akt and Erk pathways [19]. Furthermore, the presence of VEGF in the SIS ECM induced tube formation of human microvascular endothelial cells in a three-dimensional fibrin-based angiogenesis assay [46].

Cellular inflammation is divided into two separate phases: an early inflammatory phase and a late inflammatory phase. Cellular inflammation aims to establish an immune barrier against invading pathogenic organisms and phagocytose matrix debris [47]. Within 24–36 hours after injury, neutrophils and monocytes are attracted to the wound site, which is mediated by chemo-attractive agents released by degranulating platelets, to phagocytose bacteria and necrotic tissue [48]. Around 48–72 hours after injury, macrophages appear in the wound and regulate proliferation. Wound-associated macrophages are divided into classically activated M1 macrophages and alternatively activated M2 macrophages [47], which increase until day 2 to reach around 3000 cells per wound. This remains stable until day 5 and progressively decreases to steady-state levels by day 14 [49]. In the early inflammatory phase, M1 pro-inflammatory macrophages are attracted to the wound site to produce pro-inflammatory cytokines, including IL-6, TNF-α and other stimulators that accelerate the initial stages of wound healing [50]. In our study, the number of M1 macrophages in the PRP + SIS and PRP groups was higher, compared with the control and SIS groups, at day 3 post-surgery. Remarkably, activated platelets in PRP induce pro-inflammatory signalling by synthesizing IL-1β [51], and CD40 ligands released from

Downloaded from https://academic.oup.com/burnstrauma/article/doi/10.1093/burnst/tkab033/6446275 by guest on 08 June 2022

platelets can bind to CD40 on macrophages, endothelial cells and fibroblasts, inducing inflammatory events [52]. However, failure to transition from M1 to M2 phenotype can lead to a continuously negative inflammatory response and delayed wound healing [53]. To approach this problem, it is essential to promote the transition of M1 into M2 macrophages, which are typically anti-inflammatory and can secrete anti-inflammatory cytokines, such as TGF-β1 and VEGF-α, which induce fibroblast and endothelial cell proliferation [54]. In the late inflammatory phase, these cells are responsible for collagen production and angiogenesis in the wound. Our study showed that the number of M1 macrophages dramatically decreased in the PRP + SIS and PRP groups on day 7 post-surgery, while treatment with SIS alone and with the control intervention did not. In addition, our study also showed that the ratio of M2 to M1 macrophages in the PRP + SIS and PRP groups was 3.97 and 2.93 times that of the control group, respectively, and 4.56 and 3.37 times that of the SIS group, respectively, on day 7. Such effects may be attributed to apoptosis-induced platelet microparticles in PRP, which have the potential to differentiate monocytes into M2 macrophages [55]. Platelet microparticles activated by calcium can decrease TNF-α release and show low expression of CD40L, which binds to CD40 on macrophages to induce inflammatory events [56]. Furthermore, PRP can increase the expression of CD206, CD163 and CD86, as well as increase IL-10 production, all of which are M2 tissue repair macrophage-related markers [57].

Our study has several limitations. First, the difference in key parameters between PRP and PRP + SIS was minimal. One possible explanation might be that GAGs in SIS that bind chemokines and growth factors may provide a delivery system for PRP to exert a slow and persistent effect. However, healing of acute wounds in mice is short term due to self-healing. Moreover, it was difficult to observe differences between PRP and PRP + SIS. Chronic wounds and mass tissue defects may be better models to explore the effect of co-administered PRP and SIS. Second, the PRP preparation and treatment method were not standardized, which may have led to biased efficiency.

Conclusions

In conclusion, co-application of SIS and PRP to acute wounds achieves a desirable effect on modulating the macrophage immune response. In addition, co-application of SIS and PRP can accelerate wound healing and promote angiogenesis, re-epithelialization and collagen production, as well as facilitate the transition of M1 into M2 macrophages. This is a promising strategy to manage acute wound healing. Further evaluation should be performed in pig models, which have similar skin to humans and heal through physiologically similar processes [58].

Abbreviations

CD31: Endothelial cell adhesion molecule-1; DAB: 3,3′-Diaminobenz idine tetrahydrochloride; ECM: Extracellular matrix; EGF: Epidermal growth factor; GAG: Glycosaminoglycan; HA: Hyaluronic acid; H&E: Haematoxylin and eosin; IgG: Immunoglobulin G; IL-6: Interleukin-6; IOD: Integrated optical density; MOD: Mean optical density; NaCl: Sodium chloride; PDGF: Platelet-derived growth factor; PI3K: Phosphatidylinositol 3-kinase; PRP: Platelet-rich plasma; SD: Standard deviation; SIS: Small intestinal submucosa; TGF-β1: Transforming growth factor-β1; TNF-α: Tumour necrosis factor-α; VEGF: vascular endothelial growth factor; YAP: Yes-associated protein

Acknowledgements

The authors would like to thank Mr Weihong Yang (Guangzhou Sinoregen Medical Materials Co. Ltd, Guangzhou, China) for providing the SIS. We would like to thank Ms Lixia Zheng (Guangzhou Beogene Biotech Co. Ltd, Guangzhou, China) for their assistance with immunofluorescence double staining.

Funding

This research was funded by National Natural Science Foundation of China, grant number 81671924 and 81272105; National Key Research and Development Plan of China, grant number 2017YFC1103301; Health and Medical Treatment Collaborative Innovation Major Special Projects of Guangzhou, grant number 201508020253; Science and Technology Key Project of Guangdong Province, grant number 2014B020212010; Science and Technology Planning Project of Guangdong Province of China, grant number 2015B020233012; Military Medical Innovation Special Projects, grant number 18CXZ029; Zhejiang Provincial Basic Public Welfare Research Project, grant number GJ19H140001; and China's National Key R&D Programs (NKPs), grant number 2018YFB0407204.

Availability of data and materials

The data used in the current study are available upon request.

Authors' contributions

BC, GW, TF and XXL contributed to the conception and design of the study. XXL, LHHC, YY, MRP, YQD, XRZ, ZXY and CHC performed the study. XXL and LHHC organized the database. XXL, WG and LHHC carried out data analysis. XXL and WG wrote the manuscript. All authors contributed to manuscript revision, and read and approved the submitted version. Written informed consent was obtained from the volunteer for participation and publication of this study.

Ethics approval and consent to participate

The animal study was reviewed and approved by the Animal Care Committee of General Hospital of Southern Theater Command. The animal ethics approval number is 2018030601.

Conflicts of interest

All authors declare that they have no competing interests.

Downloaded from https://academic.oup.com/burnstrauma/article/doi/10.1093/burnst/tkab033/6446275 by guest on 08 June 2022

References

1. Sen CK, Gordillo GM, Roy S, Kirsner R, Lambert L, Hunt TK, *et al.* Human skin wounds: a major and snowballing threat to public health and the economy. *Wound Repair Regen*. 2009;17:763–71.
2. Broughton G, II, Janis JE, Attinger CE. Wound healing: an overview. *Plast Reconstr Surg*. 2006;117:1e-S–32e-S.
3. Etulain J. Platelets in wound healing and regenerative medicine. *Platelets*. 2018;29:556–68.
4. Martin P, Nunan R. Cellular and molecular mechanisms of repair in acute and chronic wound healing. *Br J Dermatol*. 2015;173:370–8.
5. Lumeng CN, Bodzin JL, Saltiel AR. Obesity induces a phenotypic switch in adipose tissue macrophage polarization. *J Clin Invest*. 2007;117:1917–30.
6. Hesketh M, Sahin KB, West ZE, Murray RZ. Macrophage phenotypes regulate scar formation and chronic wound healing. *Int J Mol Sci*. 2017;18:1545.
7. Daley JM, Brancato SK, Thomay AA, Reichner JS, Albina JE. The phenotype of murine wound macrophages. *J Leukoc Biol*. 2010;87:59–67.
8. Brancato SK, Albina JE. Wound macrophages as key regulators of repair: origin, phenotype, and function. *Am J Pathol*. 2011;178:19–25.
9. Zhao P, Li X, Fang Q, Wang F, Ao Q, Wang X, *et al.* Surface modification of small intestine submucosa in tissue engineering. *Regen Biomater*. 2020;7:339–48.
10. Voytik-Harbin SL, Brightman AO, Kraine MR, Waisner B, Badylak SF. Identification of extractable growth factors from small intestinal submucosa. *J Cell Biochem*. 1997;67:478–91.
11. Brown-Etris MCW, Hiles C. A new biomaterial derived from small intestine submucosa and developed into a wound matrix device. *Wounds*. 2002;14(4).
12. Kokkalis ZT, Pu C, Small GA, Weiser RW, Venouziou AI, Sotereanos DG. Assessment of processed porcine extracellular matrix as a protective barrier in a rabbit nerve wrap model. *J Reconstr Microsurg*. 2011;27:19–28.
13. Shi L, Ramsay S, Ermis R, Carson D. In vitro and in vivo studies on matrix metalloproteinases interacting with small intestine submucosa wound matrix. *Int Wound J*. 2012;9:44–53.
14. Lin HK, Godiwalla SY, Palmer B, Frimberger D, Yang Q, Madihally SV, *et al.* Understanding roles of porcine small intestinal submucosa in urinary bladder regeneration: identification of variable regenerative characteristics of small intestinal submucosa. *Tissue Eng Part B Rev*. 2014;20:73–83.
15. Iannotti JP, Codsi MJ, Kwon YW, Derwin K, Ciccone J, Brems JJ. Porcine small intestine submucosa augmentation of surgical repair of chronic two-tendon rotator cuff tears. A randomized, controlled trial. *J Bone Joint Surg Am*. 2006;88:1238–44.
16. Hodde JP, Allam R. Small intestinal submucosa wound matrix for chronic wound healing. *Wounds*. 2007;19:157–62.
17. Niezgoda JA, Van Gils CC, Frykberg RG, Hodde JP. Randomized clinical trial comparing OASIS wound matrix to Regranex gel for diabetic ulcers. *Adv Skin Wound Care*. 2005;18:258–66.
18. Dhillon RS, Schwarz EM, Maloney MD. Platelet-rich plasma therapy - future or trend? *Arthritis Res Ther*. 2012;14:219.
19. Guo SC, Tao SC, Yin WJ, Qi X, Yuan T, Zhang CQ. Exosomes derived from platelet-rich plasma promote the re-epithelization of chronic cutaneous wounds via activation of YAP in a diabetic rat model. *Theranostics*. 2017;7:81–96.
20. Kim DH, Je YJ, Kim CD, Lee YH, Seo YJ, Lee JH, *et al.* Can platelet-rich plasma be used for skin rejuvenation? Evaluation of effects of platelet-rich plasma on human dermal fibroblast. *Ann Dermatol*. 2011;23:424–31.
21. Xian LJ, Chowdhury SR, Bin Saim A, Idrus RB. Concentration-dependent effect of platelet-rich plasma on keratinocyte and fibroblast wound healing. *Cytotherapy*. 2015;17:293–300.
22. Mooren RE, Hendriks EJ, van den Beucken JJ, Merkx MA, Meijer GJ, Jansen JA, *et al.* The effect of platelet-rich plasma in vitro on primary cells: rat osteoblast-like cells and human endothelial cells. *Tissue Eng Part A*. 2010;16:3159–72.
23. Karayannopoulou M, Psalla D, Kazakos G, Loukopoulos P, Giannakas N, Savvas I, *et al.* Effect of locally injected autologous platelet-rich plasma on second intention wound healing of acute full-thickness skin defects in dogs. *Vet Comp Orthop Traumatol*. 2015;28:172–8.
24. Xu PC, Xuan M, Cheng B. Effects and mechanism of platelet-rich plasma on military drill injury: a review. *Mil Med Res* 2020;7:56.
25. Andia I, Maffulli N. Platelet-rich plasma for managing pain and inflammation in osteoarthritis. *Nat Rev Rheumatol*. 2013;9:721–30.
26. Payne WG, Wright TE, Ko F, Wheeler C, Wang X, Robson MC. Bacterial degradation of growth factors. *J Appl Res*. 2003;3:35–40.
27. Fahimi S, Abdollahi M, Mortazavi SA, Hajimehdipoor H, Abdolghaffari AH, Rezvanfar MA. Wound healing activity of a traditionally used poly herbal product in a burn wound model in rats. *Iran Red Crescent Med J*. 2015;17:e19960.
28. Du Y, Ren P, Wang Q, Jiang SK, Zhang M, Li JY, *et al.* Cannabinoid 2 receptor attenuates inflammation during skin wound healing by inhibiting M1 macrophages rather than activating M2 macrophages. *J Inflamm (Lond)*. 2018;15.
29. van den Bosch TP, Caliskan K, Kraaij MD, Constantinescu AA, Manintveld OC, Leenen PJ, *et al.* CD16+ monocytes and skewed macrophage polarization toward M2 type hallmark heart transplant acute cellular rejection. *Front Immunol*. 2017;8:346.
30. Coates M, Blanchard S, MacLeod AS. Innate antimicrobial immunity in the skin: a protective barrier against bacteria, viruses, and fungi. *PLoS Pathog*. 2018;14:e1007353.
31. Chang J, DeLillo N, Jr, Khan M, Nacinovich MR. Review of small intestine submucosa extracellular matrix technology in multiple difficult-to-treat wound types. *Wounds*. 2013;25:113–20.
32. Schallberger SP, Stanley BJ, Hauptman JG, Steficek BA. Effect of porcine small intestinal submucosa on acute full-thickness wounds in dogs. *Vet Surg*. 2008;37:515–24.
33. Akhundov K, Pietramaggiori G, Waselle L, Darwiche S, Guerid S, Scaletta C, *et al.* Development of a cost-effective method for platelet-rich plasma (PRP) preparation for topical wound healing. *Ann Burns Fire Disasters*. 2012;25:207–13.
34. Steinert AF, Noth U, Tuan RS. Concepts in gene therapy for cartilage repair. *Injury*. 2008;39:S97–113.
35. McCarrel T, Fortier L. Temporal growth factor release from platelet-rich plasma, trehalose lyophilized platelets, and bone marrow aspirate and their effect on tendon and ligament gene expression. *J Orthop Res*. 2009;27:1033–42.
36. Pintucci G, Froum S, Pinnell J, Mignatti P, Rafii S, Green D. Trophic effects of platelets on cultured endothelial cells are mediated by platelet-associated fibroblast growth factor-2 (FGF-2) and vascular endothelial growth factor (VEGF). *Thromb Haemost*. 2002;88:834–42.

Downloaded from https://academic.oup.com/burnstrauma/article/doi/10.1093/burnst/tkab033/6446275 by guest on 08 June 2022

37. Loot MA, Kenter SB, Au FL, van Galen WJ, Middelkoop E, Bos JD, *et al.* Fibroblasts derived from chronic diabetic ulcers differ in their response to stimulation with EGF, IGF-I, bFGF and PDGF-AB compared to controls. *Eur J Cell Biol*. 2002;81:153–60.
38. Xu P, Wu Y, Zhou L, Yang Z, Zhang X, Hu X, *et al.* Platelet-rich plasma accelerates skin wound healing by promoting re-epithelialization. *Burns Trauma*. 2020;8:tkaa028.
39. Rousselle P, Braye F, Dayan G. Re-epithelialization of adult skin wounds: cellular mechanisms and therapeutic strategies. *Adv Drug Deliv Rev*. 2019;146:344–65.
40. Werner S, Grose R. Regulation of wound healing by growth factors and cytokines. *Physiol Rev*. 2003;83:835–70.
41. Papakonstantinou E, Aletras AJ, Roth M, Tamm M, Karakiulakis G. Hypoxia modulates the effects of transforming growth factor-beta isoforms on matrix-formation by primary human lung fibroblasts. *Cytokine*. 2003;24:25–35.
42. Pastore S, Mascia F, Mariani V, Girolomoni G. The epidermal growth factor receptor system in skin repair and inflammation. *J Invest Dermatol*. 2008;128:1365–74.
43. Ladeira K, Macedo F, Longatto-Filho A, Martins SF. Angiogenic factors: role in esophageal cancer, a brief review. *Esophagus*. 2018;15:53–8.
44. Luo MJ, Rao SS, Tan YJ, Yin H, Hu XK, Zhang Y, *et al.* Fasting before or after wound injury accelerates wound healing through the activation of pro-angiogenic SMOC1 and SCG2. *Theranostics*. 2020;10:3779–92.
45. dela Paz NG, Walshe TE, Leach LL, Saint-Geniez M, D'Amore PA. Role of shear-stress-induced VEGF expression in endothelial cell survival. *J Cell Sci*. 2012;125:831–43.
46. Hodde JP, Record RD, Liang HA, Badylak SF. Vascular endothelial growth factor in porcine-derived extracellular matrix. *Endothelium*. 2001;8:11–24.
47. Hart J. Inflammation. 1: its role in the healing of acute wounds. *J Wound Care*. 2002;11:205–9.
48. Dale DC, Boxer L, Liles WC. The phagocytes: neutrophils and monocytes. *Blood*. 2008;112:935–45.
49. Rodero MP, Hodgson SS, Hollier B, Combadiere C, Khosrotehrani K. Reduced Il17a expression distinguishes a Ly6c(lo)MHCII(hi) macrophage population promoting wound healing. *J Invest Dermatol*. 2013;133:783–92.
50. Novak ML, Koh TJ. Macrophage phenotypes during tissue repair. *J Leukoc Biol*. 2013;93:875–81.
51. Lindemann S, Tolley ND, Dixon DA, McIntyre TM, Prescott SM, Zimmerman GA, *et al.* Activated platelets mediate inflammatory signaling by regulated interleukin 1beta synthesis. *J Cell Biol*. 2001;154:485–90.
52. Hassan GS, Merhi Y, Mourad W. CD40 ligand: a neo-inflammatory molecule in vascular diseases. *Immunobiology*. 2012;217:521–32.
53. Okizaki S, Ito Y, Hosono K, Oba K, Ohkubo H, Amano H, *et al.* Suppressed recruitment of alternatively activated macrophages reduces TGF-beta1 and impairs wound healing in streptozotocin-induced diabetic mice. *Biomed Pharmacother*. 2015;70:317–25.
54. Lucas T, Waisman A, Ranjan R, Roes J, Krieg T, Muller W, *et al.* Differential roles of macrophages in diverse phases of skin repair. *J Immunol*. 2010;184:3964–77.
55. Vasina EM, Cauwenberghs S, Feijge MA, Heemskerk JW, Weber C, Koenen RR. Microparticles from apoptotic platelets promote resident macrophage differentiation. *Cell Death Dis*. 2011;2:e211.
56. Vasina EM, Cauwenberghs S, Staudt M, Feijge MA, Weber C, Koenen RR, *et al.* Aging- and activation-induced platelet microparticles suppress apoptosis in monocytic cells and differentially signal to proinflammatory mediator release. *Am J Blood Res*. 2013;3:107–23.
57. Escobar G, Escobar A, Ascui G, Tempio FI, Ortiz MC, Perez CA, *et al.* Pure platelet-rich plasma and supernatant of calcium-activated P-PRP induce different phenotypes of human macrophages. *Regenerative Medicine*. 2018;13:427–41.
58. Sullivan TP, Eaglstein WH, Davis SC, Mertz P. The pig as a model for human wound healing. *Wound Repair Regen*. 2001;9:66–76.

Downloaded from https://academic.oup.com/burnstrauma/article/doi/10.1093/burnst/tkab033/6446275 by guest on 08 June 2022